Acta Neurochir (2012) 154:1583–1593
DOI 10.1007/s00701-012-1393-2

CLINICAL ARTICLE

Increased strain levels and water content in brain tissue after decompressive craniotomy

Hans von Holst · Xiaogai Li · Svein Kleiven

Received: 1 December 2011 / Accepted: 14 May 2012 / Published online: 1 June 2012

Abstract
Background At present there is a debate on the effectiveness of the decompressive craniotomy (DC). Stretching of axons was speculated to contribute to the unfavourable outcome for the patients. The quantification of strain level could provide more insight into the potential damage to the axons. The aim of the present study was to evaluate the strain level and water content (WC) of the brain tissue for both the pre- and post-craniotomy period.
Methods The stretching of brain tissue was quantified retrospectively based on the computerised tomography (CT) images of six patients before and after DC by a non-linear image registration method. WC was related to specific gravity (SG), which in turn was related to the Hounsfield unit (HU) value in the CT images by a photoelectric correction according to the chemical composition of brain tissue.
Results For all the six patients, the strain level showed a substantial increase in the brain tissue close to the treated side of DC compared with that found at the pre-craniotomy period and ranged from 24 to 55 % at the post-craniotomy period. Increase of strain level was also observed at the brain tissue opposite to the treated side, however, to a much lesser extent. The mean area of craniotomy was found to be 91.1 ± 12.7 cm^2. The brain tissue volume increased from 27 to 127 ml, corresponding to 1.65 % and 8.13 % after DC in all six patients. Also, the increased volume seemed to correlate with increased strain level. Specifically, the overall WC of brain tissue for two patients evaluated presented a significant increase after the treatment compared with the condition seen before the treatment. Furthermore, the Glasgow Coma Scale (GCS) improved in four patients after the craniotomy, while two patients died. The GCS did not seem to correlate with the strain level.
Conclusions We present a new numerical method to quantify the stretching or strain level of brain tissue and WC following DC. The significant increase in strain level and WC in the post-craniotomy period may cause electrophysiological changes in the axons, resulting in loss of neuronal function. Hence, this new numerical method provides more insight of the consequences following DC and may be used to better define the most optimal size and area of the craniotomy in reducing the strain level development.

Keywords Traumatic brain injury · Stroke · Decompressive craniotomy · Strain level · Water content

H. von Holst
Section of Neurosurgery, Division of Clinical Neuroscience,
Karolinska Institutet,
SE-171 76 Stockholm, Sweden

H. von Holst · X. Li · S. Kleiven
Division of Neuronic Engineering, School of technology
and Health, Royal Institute of Technology (KTH),
Stockholm, Sweden

H. von Holst (✉)
Department of Neurosurgery, Karolinska University Hospital,
SE-171 76 Stockholm, Sweden
e-mail: hans.vonholst@karolinska.se

Introduction

Traumatic brain injury (TBI) is a heavy burden in a global perspective [53], which holds true also for patients with stroke. Except for general and neurological intensive care treatment, patients with the most severe TBI and stroke are treated with so-called decompressive craniotomy (DC) to reduce the intracranial pressure (ICP) caused by cerebral swelling [1, 38]. The use of DC has increased, although a

complete consensus on its effectiveness has not been fully achieved [42, 47, 50]. A retrospective and prospective analysis including more than 155 patients was presented recently showing no convincing difference in outcome for patients treated with either conservative intensive care or with DC [14], and a debate arose on how to interpret the data in clinical practice [39, 46, 50].

DC allows expansion of the swollen brain outside the skull [14, 42], which causes stretching of the axons. Stretching of axons is thought to result in diffuse axonal injury (DAI) during the rapid deformation of brain tissue following an impact [13, 26, 40]. Axonal injury was found in dynamic axonal stretch experiments [12, 41, 45]. Bain et al. [2] demonstrated in an animal model that a strain level of approximately 21 % will elicit electrophysiological changes, while a strain of approximately 34 % will cause morphological signs of damage to the white matter. Using a stretching model of the sciatic nerve, Fowler et al. [19] concluded that even minimal tension, if maintained for a significant amount of time, may result in neuronal functional loss. It should therefore be expected that the central nervous system (CNS) will also sustain potential damage under a long duration of stretch such as in the post-craniotomy stage. As has been suggested, axonal stretch may contribute to the unfavourable outcome of the craniotomy patients [14].

Early studies using experimental animal models found that DC may cause worsening of cerebral oedema [15, 20]. A similar effect of DC has been reported by a recent study [44]. However, other research groups revealed contradictory results that reduced brain oedema formation was found in the group treated with DC [35, 48, 56]. The Hounsfield unit (HU) value from computerised tomography (CT) images was closely related to the severity of brain oedema, which appear as low-density areas on CT images due to excess water accumulation [24, 36, 37]. Although the occurrence of brain oedema can be demonstrated with CT scans, the quantitative determination of water content (WC) could play an important role in the evaluation of the severity of brain oedema and the monitoring of the treatment efficiency.

Thus, the aim of the present study was to clinically evaluate earlier experimental studies by the presentation of a new software image method which analyses the strain level and WC in the brain tissue using the patient's CT images before and after DC.

Patients and methods

Patient information

Six patients aged 25–61 (mean 45±13.8 years) were included in this study and treated with DC due to trauma in one patient and to stroke in five patients. The Glasgow Coma Scale (GCS) and CT were evaluated both before and after the DC.

Quantification of brain tissue deformation in pre-craniotomy and post-craniotomy period

An image registration method was used to investigate the brain deformation retrospectively based on the CT images of the patients before and after DC. A non-linear registration method, the Diffeomorphic Demons algorithm [51] implemented in the open-source software Slicer 3D [34], was used, which allows accounting for localised distortion and large deformation while simultaneously preserving the topology [51]. Due to the compression of the ventricular system, brain tissue was deformed from a healthy stage to the pre-craniotomy state. Thus, both the strain level at pre-craniotomy and post-craniotomy images needs to be quantified which makes it necessary to obtain a healthy brain image before analysing the TBI or stroke in the patient. Since a pre-TBI or stroke image of each patient is unavailable, an image registration method was used to recover a healthy brain image of the patient before the TBI and stroke. The magnetic resonance (MR) images of a healthy volunteer at a similar age were used and which should give a reasonable approximation for the recovered ventricular shape due to the fact that ventricle volumes are age-dependent [27]. The MR images were then morphed to the patient's CT image at the pre-craniotomy state according to the cranial shape (*see* [28] for more detail). The morphing result is the recovered healthy brain with one slice having a zero strain level presented as a comparison for patient MC (Fig. 4, *Healthy brain*). The assumption underlying this approach is that all normal brains, at least at a certain level of representation, have a similar topological structure, but may differ in shape details [3].

The ventricles and the outer layer of the brain were segmented as binary images for the recovered healthy brain, pre- and post-craniotomy CT images. In order to apply Demons registration, a rigid registration step was used to centre the images about the same point. The displacement field was then obtained through the Diffeomorphic Demons registration. From the calculated displacement field representing the motion of the brain tissue due to DC, a quantitative description of the tissue deformation in the brain following the craniotomy can be derived in the form of the finite Lagrange strain tensor [21, 23]. Different scalar indices can be derived from the strain tensor, especially, the first principal strain, which represents the maximum stretching was used to describe the stretching of brain tissue. Strain quantification by image registration has been used in different organs such as the lung and the heart [6, 21, 22, 33, 52]. This method has also been used to study brain tissue deformation during mild skull impact on healthy volunteers [4, 18].

Assessment of the registration agreement

There are many possible transformations that could match a set of identifiable image features [16]. With all the possibilities, it is important to check how physically plausible the registration result is for the particular applications. For data without ground truth, the mean square difference (MSE), Harmonic energy and Jacobian determinant have been used to assess the registration quality [25]. The determinant of the Jacobian matrix of the deformation field, j, represents the local relative tissue volume change throughout the brain. Where $j<1$, local contraction is implied, $j=1$ implies no volume change and $j>1$ implies local expansion [23]. The brain tissue region with largest j value is located around the ventricular system and at the site of craniotomy. The Jacobian determinant of the deformation field overlayed with the deformed frame showing how the inner brain structure was deformed for patient MC is demonstrated in Appendix 1.

Mapping the water content

The extraction of WC is based on a relationship between WC and specific gravity (SG) [32], which could be obtained from the Hounsfield unit (HU) value in the CT images by a photoelectric correction value ΔH_p [9, 10, 36] according to the chemical composition and the X-ray energy. SG then serves as a bridge to connect the HU value from CT image with that of the WC. In order to make the HU values from different images comparable, both pre- and post-craniotomy images were calibrated using a two-point calibration method using CSF and air as references [7]. Different equations apply for grey and white matter due to the chemical composition difference, which makes it necessary to segment the images. This was performed by using an atlas-based method [11]. Morphing a segmented brain atlas to the patient brain according to the cranial and lateral ventricle shape and the morphed template gives the segmented image. The detailed steps of analysing WC are described in Appendix 2.

Results

The results of strain level and WC are presented separately in the following sections.

Strain level overview

The quantified strain levels at both pre- and post-craniotomy for all the six patients are presented in Fig. 1. Craniotomy allows brain tissue to expand outside the skull as shown from the CT images at the post-craniotomy period (Fig. 1, *row 2*). The maximum motion of the brain tissue occurred around the centre of the craniotomy and ranged from 7 to 21 mm. A similar strain pattern is seen for all patients, but to a different extent. In the pre-craniotomy brain, the strain level is large around the ventricular system, which makes the neurons around the ventricles either stretched or compressed (Fig. 1, *row 3*). For patient VM, the pre-craniotomy image looked normal, thus no deformation occurred, and a slice with zero strain at pre-craniotomy was plotted. Following DC, the strain level increased substantially at the treated side compared with that before the treatment (Fig. 1, *row 4*). Also, the strain is more widespread compared with the pre-craniotomy. Moreover, an increase in strain level on the opposite side of the DC was also observed, however, to a much lesser extent compared with the treated side. Thus, the DC results in a substantially increased strain level towards the treated side simultaneously with an increased strain level in the expanded brain tissue area itself. The maximum strain level was localised around the skull edge of the DC, indicating that the neurons in this area were under serious stretching (Fig. 1, *row 5*).

The evaluation of axonal stretching at the treated part of craniotomy is of great interest since it has been suggested to contribute to the unfavourable outcome for the patients [14]. Thus, the average strain level of brain tissue expanded outside the skull was evaluated for both the pre- and post-craniotomy stages with the results presented in Fig. 2 (*left*). For all the patients, the average strain level at the expanded brain tissue increased significantly after craniotomy ranging from 24 to 55 %. The GCS improved in four patients after the craniotomy, while two patients died (Fig. 2, *right*). The GCS did not seem to correlate with the strain level.

Craniectomy sizes were measured in the six patients based on postoperative CT scans following the method defined in [54]. The CT scanning was re-sampled in 8-mm-slice thickness without gap or overlap. Distance between the posterior and anterior margins of the bone defect was measured on each slice using the inner table of the skull bone. The total craniotomy size of DC was calculated by multiplying this value by the slice thickness and adding all results. The mean craniotomy size was 91.1 ± 12.7 cm^2 and it ranged from 70.1 to 107.2 cm^2. In general, a larger craniotomy size tends to lead to a smaller average strain level development at the brain tissue that expanded outside the skull (Fig. 3, *left*). A largest strain level development was found in Patient VM with a smallest craniotomy size.

DC allows brain tissue to expand outside the skull, thus causes an increase in brain tissue volume. The increased volume was calculated based on the segmented CT images for both pre- and post-craniotomy images by subtracting the segmented cranial shape at post-craniotomy from the pre-craniotomy images. Based on this subtraction, the relative volume increase in percentage in the six patients was calculated. The brain tissue volume increased after DC in all six patients ranging from 27 ml to 127 ml corresponding to

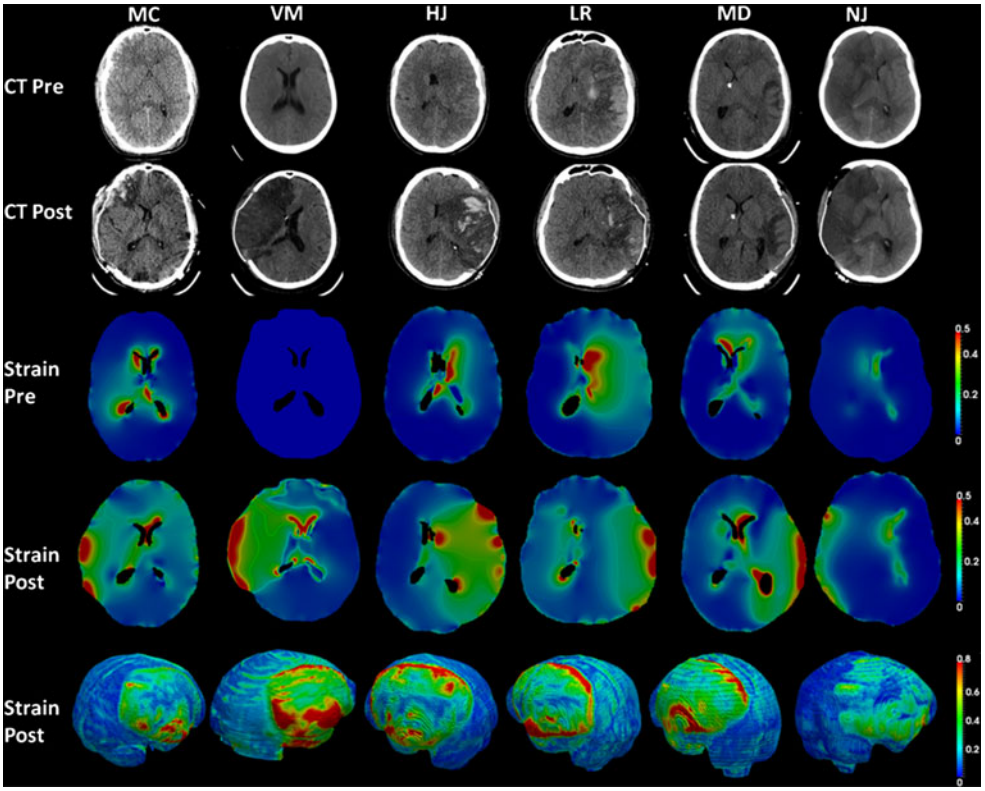

Fig. 1 Strain levels quantified for all the six patients. A representative axial slice of the CT images at pre-craniotomy period (*row 1*). A representative axial slice of the CT images at post-craniotomy period (*row 2*). A representative axial slice of the quantified strain level is shown at pre-craniotomy (*row 3*) and post-craniotomy period (*row 4*). Contour of strain level at brain tissue abutting the skull base at post-craniotomy period (*row 5*)

1.65 % and 8.13 %, respectively. Also, despite the small number of patients, the relative volume increase [i.e. ΔV (%)] seems to correlate with increased strain level (Fig. 3, *right*). A larger volume increase in general, tends to cause a larger strain level increase (Fig. 3, *right*).

Comparison of the strain levels in different regions

In an effort to exemplify the different strain levels in the brain tissue, the strain level was further analysed for patient MD by plotting the strain along the cross-lines before and after DC (Fig. 4a–c) showing a significant influence of the treatment has on the strain level.

The increased strain level differs significantly depending on where the analysis is taking place. The strain level in the vicinity of the DC shows a higher level after the treatment (Fig. 4a, b), and other areas with a longer distance from the DC also presents an increase of strain level, however, to a lesser extent (Fig. 4c). Note that in order to compare the same brain tissue point, the strain level at pre-craniotomy stage was mapped to the post-craniotomy space by the displacement field relating these two states.

Water content

Comparison of the water content in different regions

The water content was analysed more extensively in two patients (MC and VM). The quantified water content for patient MC is presented in Fig. 5. In comparison to normal conditions of WC, which are around 70 % for white matter and 80 % for grey matter [17], the WC shows a slightly increased concentration in the brain tissue of the TBI patient after the DC (Fig. 5, *lower row*), reaching a WC of up to 90 % in some areas of the brain tissue.

When comparing the WC before and after the treatment, the increased WC is more obvious in the white matter of the frontal lobe where a haemorrhage was seen from the CT

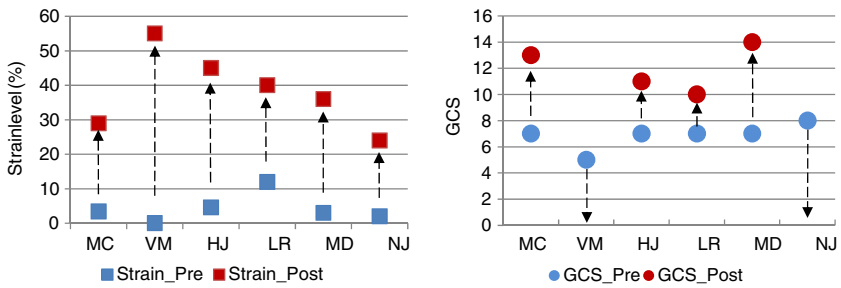

Fig. 2 Average strain level at regions of brain tissue expanded outside the skull for the six patients (*left*). Clinical outcome (i.e. GCS) after decompressive craniotomy (*right*)

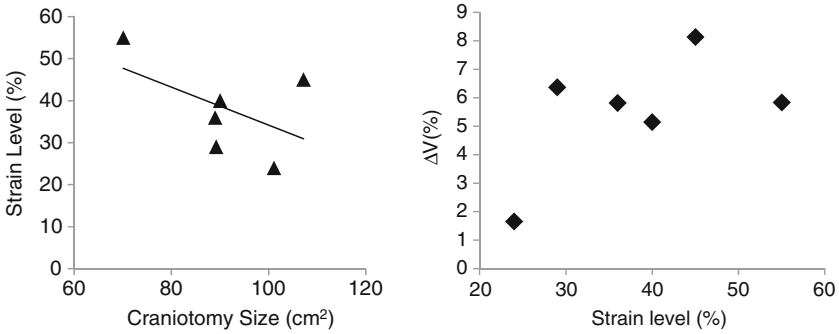

Fig. 3 Craniotomy size with average strain level of brain tissue that expanded outside the skull (*left*). Average strain level of brain tissue that expanded outside the skull with the relative volume increment for the six patients (*right*)

image (Fig. 1, *row 2*, *column MC*). For other parts of the brain, the increased WC is distributed in a relatively similar way in both hemispheres regardless of the area of DC. A probability density function (PDF) was used to depict the relative frequency at a given WC level. The PDF provided a profile of WC distribution of the entire brain, which was characterised by two distinct peaks, one for white matter and one for grey matter (Fig. 5). The development of oedema is characterised by more voxels at higher WC, which is equivalent to a shift of the profile to the right. The average WC in the whole brain is significantly increased after the DC compared with that seen before the treatment (Fig. 5). The average WC of white matter had increased ($P<0.001$) from 70.6 %±5.7 % to 73.1 %±5.9 %, and for grey matter ($P<0.001$) from 82.5 %±3.6 % to 84.5±5.9 %, respectively (mean ± standard deviation).

For patient VM, compared with the pre-craniotomy period, the WC increment showed clear preferences at the treated hemisphere compared with the opposite side (Fig. 6). The average WC in the whole brain is

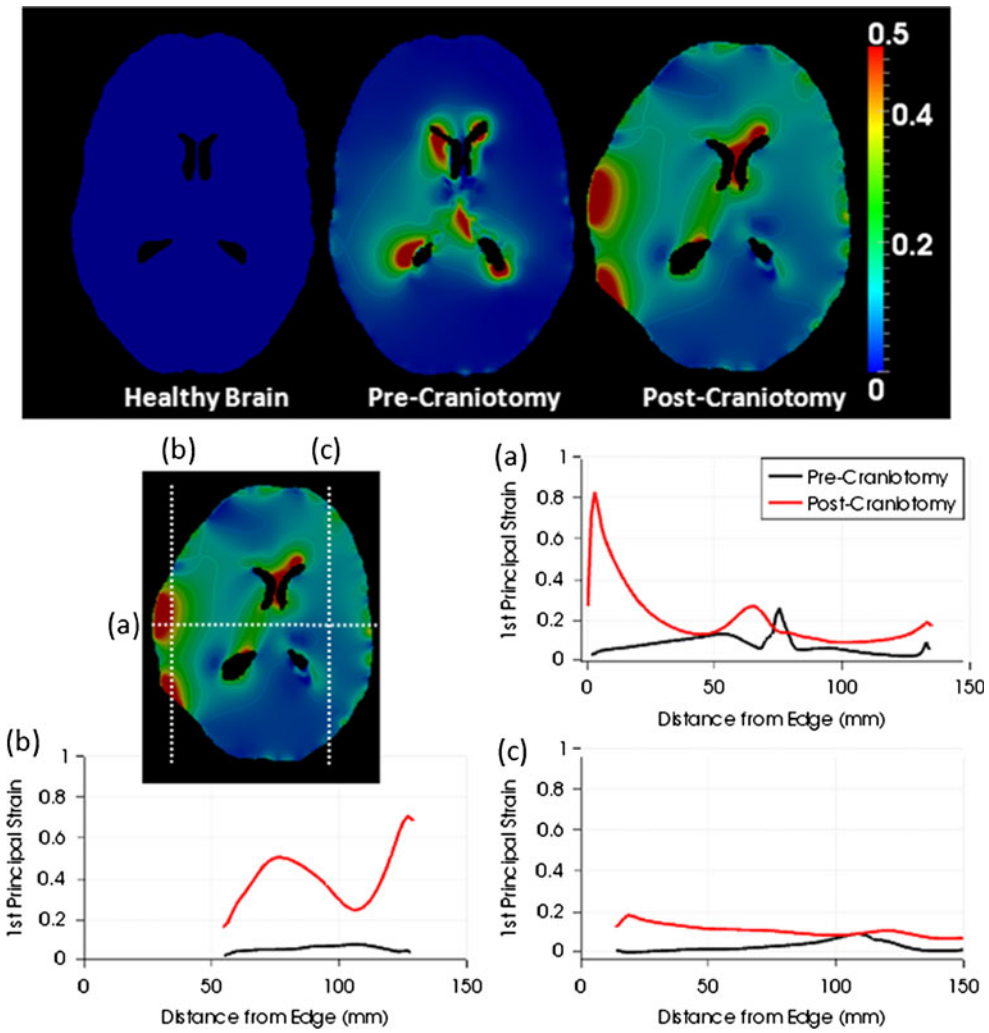

Fig. 4 Strain distribution at a representative axial slice in the healthy, pre-craniotomy and post- craniotomy period (*upper row*). Evaluation of the strain levels before and after treatment along the cross-lines in three different areas of the brain tissue (**a**–**c** *lower row*)

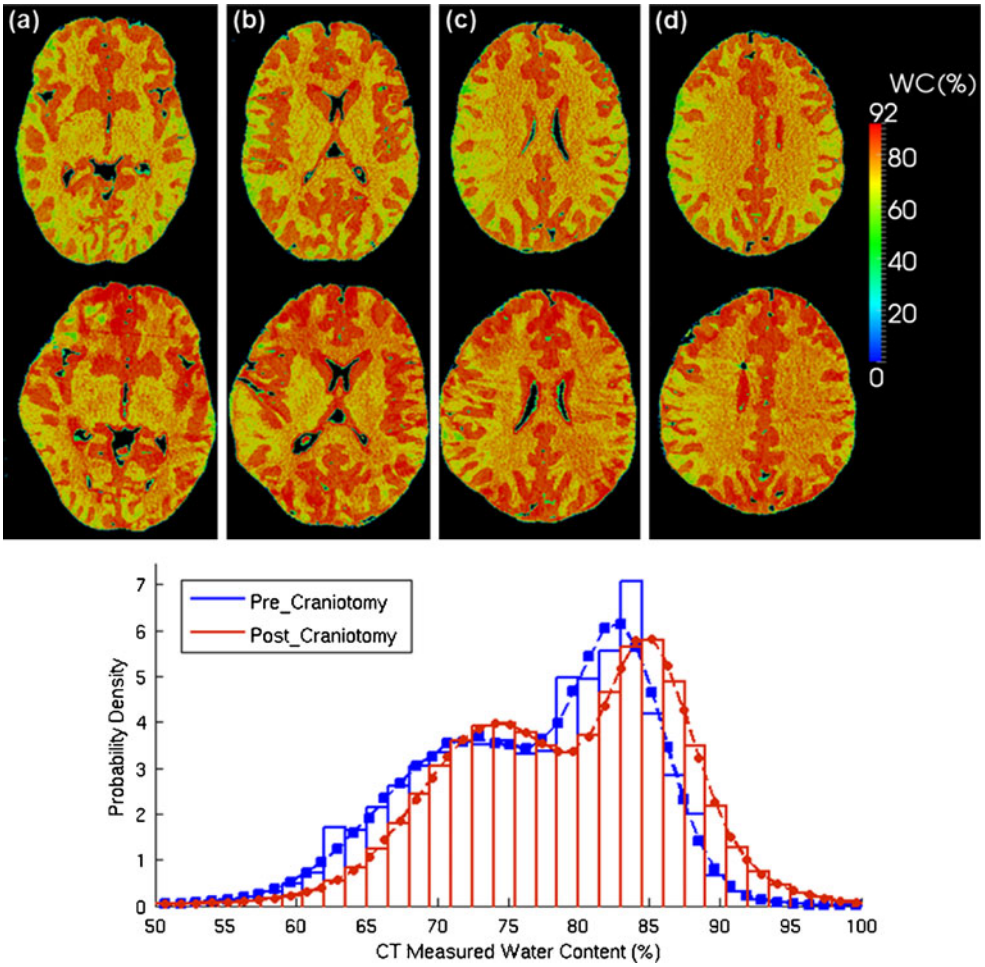

Fig. 5 Quantitative water content (WC) maps in four consecutive transverse slices through the brain in the pre-craniotomy (*upper row*) and post-craniotomy (*lower row*) period for patient MC. The probability density function of WC for the entire brain shows a shift of WC toward a higher level in the post-craniotomy period

significantly increased after the DC compared with that seen before the treatment. The average WC of white matter had increased ($P<0.001$) from 73.2 %±3.7 % to 76.0 %±6.2 %, and for grey matter ($P<0.001$) from 84.5 %±3.0 % to 86.3 %±4.5 %, respectively (mean ± standard deviation).

Discussion

The recommended treatment following TBI and stroke is predominately based on clinical practice and personal experience. DC may lead to an improvement in physiological parameters, such as an effective decrease in ICP [14] and also to increase in cerebral blood flow (CBF) velocity [47]. However, the impact of this procedure on clinical outcome and social rehabilitation has not been clearly established. Both the strain level as well as WC in the brain tissue is of major importance when DC is used following severe TBI. In this study, we have proposed a new method to quantify the strain levels and WC from CT images in the entire brain tissue following DC. The substantially increased strain level and WC after DC may jeopardise the axonal function in a negative way. We found that there is a surprisingly high level of strain in the brain tissue due to craniotomy and especially in regions where the brain tissue gets in close contact with the edges of the opened skull bone where the brain tissue is seriously stretched (Fig. 1, *row 6*). This might result in irreversible dysfunction of the brain tissue in those regions. The stretch of axons in the cerebral tissue fibres may very well lead to disruption of axonal transport and metabolism [30]. The increased strain level in the most peripheral of the treated side is probably caused by the lower resistance of the dura mater compared with the skull bone. This allows larger brain tissue expansion compared with tissue adjacent to the bones of the skull, which causes distortion of brain tissue at this part. Thus, the size and shape of the edges of the skull bone defect are important factors to be considered when performing the surgical procedure. The craniotomy size performed in clinics could differ from one patient to another, and a large enough craniotomy size was suggested to be important for a better neurological outcome [54], which is confirmed in the present study with regards to the strain level increase in the vicinity of the skull edges. Also, we propose that it is quite possible to reduce the sharpness of the skull edges by

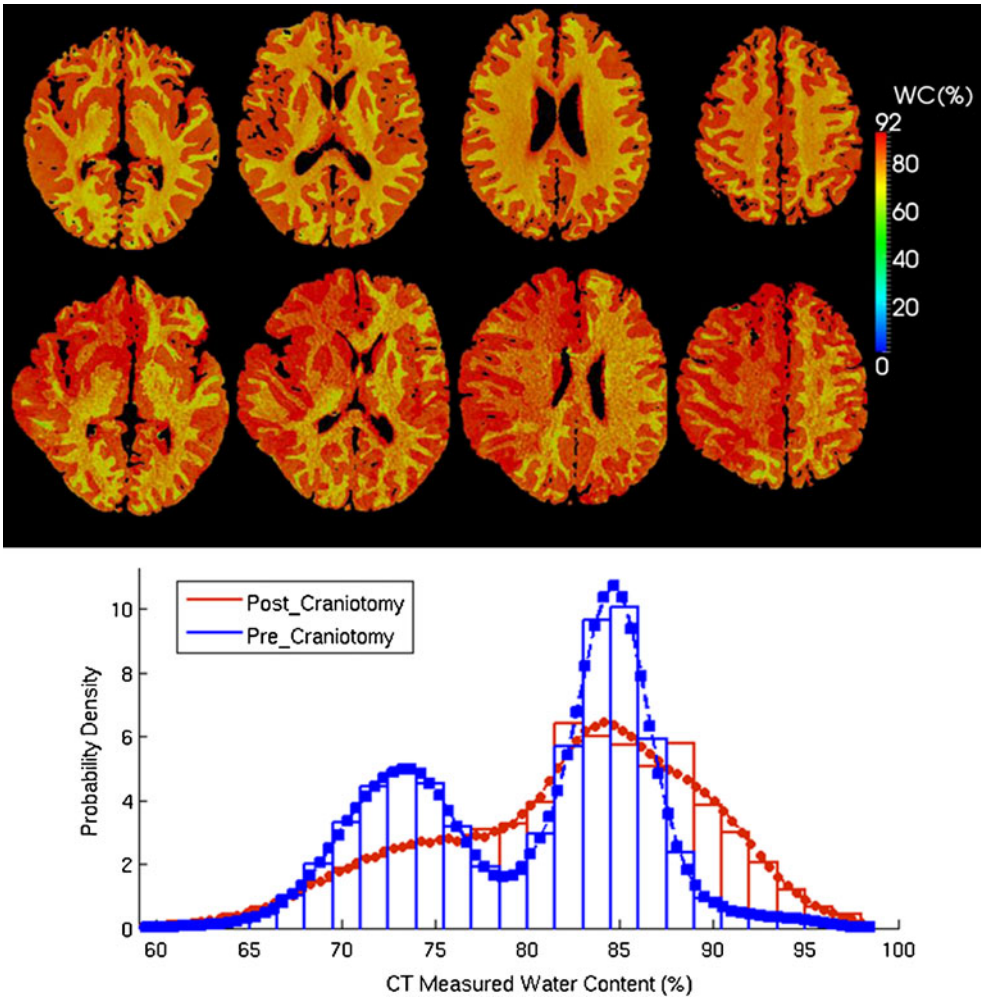

Fig. 6 Quantitative water content (WC) maps for four consecutive transverse slices through the brain in the pre-craniotomy (*upper row*) and post-craniotomy (*lower row*) period for patient VM. The probability density function for the entire brain shows a shift of WC toward a higher level in the post-craniotomy period

changing the angles of the bone flap at the time of craniotomy. Further, a larger craniotomy size tends to lead to a smaller strain level development at the brain tissue that expanded outside the skull (Fig. 3, *left*). This suggests that a larger craniotomy size should be considered to improve the metabolic conditions of the neuronal tissue [54].

Based on the present results, it has been shown that the new image method could be used to assess and visualise the strain level caused by the DC and it is suggested that further biomechanical models should be developed for preplanning of where the DC should be performed on the skull, aiming at reaching the least strain level in the brain tissue while simultaneously lowering the ICP.

The increased brain tissue strain level was up to 80 %, and 120 % for patient MC and patient VM respectively, at some regions of the treated part. To give a physical interpretation, a strain level of 120 % indicates that brain tissue has been stretched to 2.2-times its original length. When this deformation reaches a critical point or threshold, it will initiate a biochemical response, thereby causing the neuronal injury which was speculated to contribute to the unfavourable outcome of DC patients [14]. Earlier studies found that a strain level of 5 % will alter neuronal function, while 10 % can cause cell death in rapid axonal stretching models [55]. Under slow loading rates, with duration of minutes, the axons could tolerate much higher strain levels [45]. However, in the case of axonal stretch for the post-craniotomy stage under which the axons are under a sustained static stretching for days and even weeks, the potential damage due to axonal stretching remains unclear. Using a model of sciatic nerve stretch, Fowler et al. [19] have reported that even minimal tension, if maintained for a significant amount of time, may result in loss of neuronal function. A similar pattern should be expected also for the central nervous system, resulting in a sustainable potential damage under long duration stretch as in the post-craniotomy situation. The question how this high strain level of brain tissue found at the post-craniotomy stage affects the neuronal function and the outcome of the patient is unclear and is waiting for further experimental studies.

It has been suggested that DC not only includes the removal of a part of the skull bone but also part of the dura should be opened, aiming at allowing the brain tissue to move out of the skull even further. With such a high strain

level found in this simulation, partial opening of the dura may even further increase the strain level in this region, thereby jeopardising the neuronal metabolism to an unacceptable level. DC has indeed reduced the number of deaths, while the number of vegetative stages has increased. One possible explanation is that DC reduces the ICP, while it reduces the neuronal metabolism by the increased strain level. Thus, based on the present results one can tentatively suggest that allowing a further extension of brain tissue will result in even higher numbers of vegetative stages among these patients.

The clinical condition defined with the GCS before and after DC treatment did not correlate with the strain level. This is not a surprise as the clinical condition is dependent on several different factors. Size of injury is one important aspect, while TBI and stroke are two different causes of illness. TBI includes an external kinetic impact of different energy supply transferred to the whole brain, while stroke, as an original illness, is an internal impact. Both diseases may develop in different ways, resulting in different consequence. The anatomical localisation is another important aspect to explain why it should not be so easy to find any correlation between GCS and strain level. Nevertheless, the importance of defining the strain level on an individual basis is that it may be part of an answer to a patient's clinical outcome.

The post-craniotomy increased WC in the two exemplified patients after treatment compared with pre-craniotomy was found to be 2.5 % and 2.0 % for white matter and grey matter, respectively for patient MC. while the corresponding values were 2.8 % and 1.8 % for patient VM. This is in line with the clinical findings that DC may lead to worsening of cerebral oedema [15, 20, 44] which may develop over days [43]. It is worth noting that both patients evaluated in this study showed higher WC at the post-craniotomy stage. However, it is not known whether this development could be attributed to the DC. In the post-craniotomy period, most of the brain tissue was allowed to expand and it is more obvious at the areas close to the treated part. From a mechanical point of view it is clear that with an increased volume, more space is available to accumulate more fluid, and the WC increment found in patient VM is as expected. For patient MC, however, there is no preference of increased WC at the treated part compared with the opposite hemisphere, which shows a similar distribution. This should indicate that the increased WC due to mechanical expansion caused by DC played a limited role in this case. Instead, the development of brain oedema is a complex consecutive pathological process which depends on the type of primary lesions and associated conditions [49]. Although the data set of WC with only two patients exemplified included in this study did not allow conclusions about the impact of DC on the development of brain oedema, the approach proposed here could be readily extended to include more patient data in future studies.

WC of the oedematous brain is one of the major determinants of CT attenuation and the HU value from CT images was reported to be closely related with WC [36]. A lower HU value, which shows reduced density on the CT image, usually represents an increment of WC. However, the correlation of the HU value with the WC is complex, and there is no single relationship between WC and HU value. For example, despite the higher WC, grey matter has a higher HU value than white matter and thus presents brighter in the CT images. In order to solve this problem, we proposed a method by firstly connecting HU value with that of SG with different photoelectric correction values for grey and white matter according to their chemical composition respectively [36]; SG in turn is related to WC [29], thereby establishing a relationship between WC and the HU value from the CT images. The SG-WC relationship used was taken from Marmarou et al. [29], but a slightly different equation was reported by Boethe et al. [8]. Thus, although the absolute WC obtained from the two examples in this study was reasonable, the results should be interpreted with caution since they were dependent on the SG-WC equation used. Nevertheless, since the same set of equations was used for pre- and post-craniotomy images, the conclusions drawn on WC increment is independent of the choice of SG-WC equations.

It is difficult to correlate the HU value from one scanner to another, due to different scanning parameters, such as the tube current (mA), tube voltage (kV), reconstruction kernel and slice thickness. However, the mean HU value, which is an intrinsic property of the material being examined, is mainly dependent on the photoelectric energy (i.e. kV settings) [5], other aforementioned parameters only affect the image quality, and some images may be noisier than others. Since both pre- and post-craniotomy images for both exemplified patients were taken at 120 kV, this makes HU values from these images comparable. Furthermore, a two-point calibration using CSF and air [7] were performed as this should eliminate most of the inter-scanner calibration problem.

Conclusions

The present results show that it is possible to evaluate the strain level of neuronal tissue following DC. Also, it is suggested that further biomechanical models should be eveloped to predict the strain level already before the treatment. Such a prediction may support the neurosurgical procedure where to place and how to design the craniotomy to find the least strain level development. Although it is sometimes not possible to avoid DC for severe TBI and stroke patients with increased ICP, awareness and a better understanding of the DC reducing the ICP but simultaneously increase the strain level, thereby jeopardising the cerebral

metabolism in the neuronal tissue should promote the prevention of further damage to the brain.

Acknowledgements We would like to acknowledge financial support provided by the Swedish Research Council D.nr. 621-2008-3400, the Swedish Governmental Agency for Innovation Systems (VINNOVA), and the Chinese Council Scholarship (CSC) for the second author.

Conflicts of interest None.

Appendix 1

Jacobian determinant map of the displacement field

The Jacobian determinant of the deformation field is overlayed with the deformed frame showing how the inner structure of the brain tissue was deformed (Fig. 7).

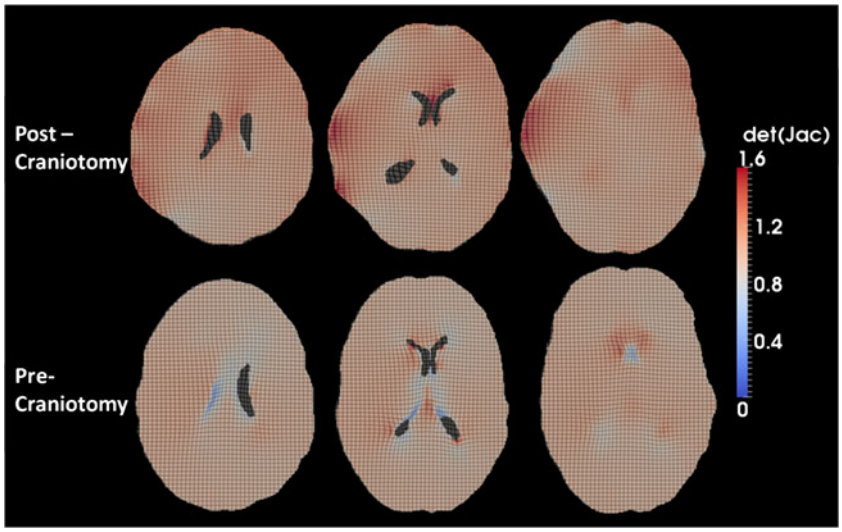

Fig. 7 Jacobian determinant map of the displacement field overlayed with the deformed frame shows how the inner structure of the brain tissue was deformed at different axial sections for patient MC

Appendix 2

Analysis of water content

Analysis of WC was performed in the following steps:

- The relationship between SG and WC was obtained by using experimental data from [29] according to the equation derived in [32]. For white matter, $WC = 784.93/SG - 684.93$, and for grey matter $WC = 484.62/SG - 384.62$ [29].
- Photoelectric correction ΔH_p was calculated in order to relate SG with the HU value. $SG = n/n_w(1 + H_c/1000)$, and $H_c = HU - \Delta H_p$, where n is the number of nucleons per electron for the tissue and n_w is the number of nucleons per electron for water (n_w=1.8125) [36]. According to the chemical composition for white matter and grey matter from [10], the values of n are near identical for white and grey matter with n_WM=1.8125 and n_GM=1.8121 for white and grey matter respectively. The HU and H_c values for normal white and grey matter were calculated from the mass attenuation coefficients obtained from the Photon Cross Sections Database [5] at 70 keV (the approximated effective energy corresponding to the 120 kV tube voltage [31] which was used for both the pre- and post-craniotomy CT images) by adding the coefficient of each element weighted by the composition fraction. The obtained values are ΔH_p_WM=−1.386 and ΔH_p_WM=4.0098. These values are very close to the value in [10] at 80 keV energy level.
- HU values were calibrated using the average value of CSF ($H_{\_aveCSF}$) from pre and post-craniotomy CT images and air (HU=−1,000) as reference. After calibration, the HU value for CSF becomes $H_{\_aveCSF}$ and −1,000 for air for both pre- and post-craniotomy images.

References

1. Aarabi B, Hesdorffer DC, Ahn ES, Aresco C, Scalea TM, Eisenberg HM (2006) Outcome following decompressive craniectomy for malignant swelling due to severe head injury. J Neurosurg 104:469–479
2. Bain AC, Meaney DF (2000) Tissue-level thresholds for axonal damage in an experimental model of central nervous system white matter injury. J Biomech Eng 122:615–622

3. Bajcsy R, Kovacic S (1989) Multiresolution elastic matching. Comput Vis Graph 46:1–21
4. Bayly PV, Cohen TS, Leister EP, Ajo D, Leuthardt EC, Genin GM (2005) Deformation of the human brain induced by mild acceleration. J Neurotrauma 22:845–856
5. Berger M, Hubbell J, Seltzer S, Coursey J, Zucker D (2011) Xcom: Photon cross sections database, nist standard reference database 8 (xgam). http://www.nist.gov/pml/data/xcom/index.cfm. Accessed 20 Oct 2011
6. Boldea V, Sarrut D, Clippe S (2003) Lung deformation estimation with non-rigid registration for radiotherapy treatment. Proceedings of MICCAI 2003. Lect Notes Comput Sci 2878:770–777
7. Boris P, Bundgaard F, Olsen A (1987) The CT (Hounsfield unit) number of brain tissue in healthy infants. Childs Nerv Syst 3:175–177
8. Bothe HW, Bodsch W, Hossmann KA (1984) Relationship between specific gravity, water content, and serum protein extravasation in various types of vasogenic brain edema. Acta Neuropathol 64:37–42
9. Brooks RA (1977) A quantitative theory of the hounsfield unit and its application to dual energy scanning. J Comput Assist Tomogr 1:487–493
10. Brooks RA, Di Chiro G, Keller MR (1980) Explanation of cerebral white–gray contrast in computed tomography. J Comput Assist Tomogr 4:489–491
11. Cabezas M, Oliver A, Lladó X, Freixenet J, Bach Cuadra M (2011) A review of atlas-based segmentation for magnetic resonance brain images. Comput Methods Prog Biomed 104:e158–e177
12. Chung RS, Staal JA, McCormack GH, Dickson TC, Cozens MA, Chuckowree JA, Quilty MC, Vickers JC (2005) Mild axonal stretch injury in vitro induces a progressive series of neurofilament alterations ultimately leading to delayed axotomy. J Neurotrauma 22:1081–1091
13. Cloots RJH (2011) Micromechanics of diffuse axonal injury: influence of axonal orientation and anisotropy. Biomech Model Mechanobiol 10:413–422
14. Cooper DJ, Rosenfeld JV, Murray L, Arabi YM, Davies AR, D'Urso P, Kossmann T, Ponsford J, Seppelt I, Reilly P, Wolfe R (2011) Decompressive craniectomy in diffuse traumatic brain injury. N Engl J Med 364:1493–1502
15. Cooper PR, Hagler H, Clark KW, Barnett P (1979) Enhancement of experimental cerebral edema after decompressive craniectomy: implications for the management of severe head injuries. Neurosurgery 4:296–300
16. Crum WR, Griffin LD, Hill DLG, Hawkes DJ (2003) Zen and the art of medical image registration: correspondence, homology, and quality. NeuroImage 20:1425–1437
17. Fatouros PP, Marmarou A (1999) Use of magnetic resonance imaging for in vivo measurements of water content in human brain: method and normal values. J Neurosurg 90:109–115
18. Feng Y, Abney TM, Okamoto RJ, Pless RB, Genin GM, Bayly PV (2010) Relative brain displacement and deformation during constrained mild frontal head impact. J R Soc Interface 7:1677–1688
19. Fowler SS, Leonetti JP, Banich JC, Lee JM, Wurster R, Young MRI (2001) Duration of neuronal stretch correlates with functional loss. Otolaryngol Head Neck Surg 124:641–644
20. Gaab M, Knoblich OE, Fuhrmeister U, Pflughaupt KW, Dietrich K (1979) Comparison of the effects of surgical decompression and resection of local edema in the therapy of experimental brain trauma. Pediatr Neurosurg 5:484–498
21. Gee J, Sundaram T, Hasegawa I, Uematsu H, Hatabu H (2003) Characterization of regional pulmonary mechanics from serial magnetic resonance imaging data. Acad Radiol 10:1147–1152
22. Hartkens T, Hill DLG, Castellano-Smith AD, Hawkes DJ, Maurer CR Jr, Martin AJ, Hall WA, Liu H, Truwit CL (2003) Measurement and analysis of brain deformation during neurosurgery. IEEE Trans Med Imaging 22:82–92
23. Holzapfel GA (2000) Nonlinear solid mechanics: a continuum approach for engineering. Wiley, Chichester
24. Ito U, Reulen HJ, Huber P (1986) Spatial and quantitative distribution of human peritumoural brain oedema in computerized tomography. Acta Neurochir (Wein) 81:53–60
25. Johnson H, Zhao Y (2009) Brainsdemonwarp: An applicaton to perform demons registration. http://www.insight-journal.org/browse/publication/312. Accessed 20 Nov 2011
26. Kleiven S (2007) Predictors for traumatic brain injuries evaluated through accident reconstructions. Stapp Car Crash J 51:1–35
27. Kruggel F (2006) Mri-based volumetry of head compartments: normative values of healthy adults. NeuroImage 30:1–11
28. Li X (2012) Finite element and neuroimaging techniques to improve decision-making in clinical neuroscience. PhD thesis, Royal Institute of Technology (KTH)
29. Marmarou A, Tanaka K, Shulman K (1982) An improved gravimetric measure of cerebral edema. J Neurosurg 56:246–253
30. Maxwell WL, Irvine A, Adams JH, Gennarelli TA, Tipperman R, Sturatis M (1991) Focal axonal injury: the early axonal response to stretch. J Neurocytol 20:157–164
31. McCollough C, Cody D, Edyvean S, Geise R, Gould B, Keat N, Huda W, Judy P, Kalender W, McNitt-Gray M et al (2008) The measurement, reporting, and management of radiation dose in CT, technical report 96. American Association of Physicists in Medicine, College Park
32. Nelson SR, Mantz ML, Maxwell JA (1971) Use of specific gravity in the measurement of cerebral edema. J Appl Physiol 30:268–271
33. Phatak NS, Maas SA, Veress AI, Pack NA, Di Bella EVR, Weiss JA (2009) Strain measurement in the left ventricle during systole with deformable image registration. Med Image Anal 13:354–361
34. Pieper S, Halle M, Kikinis R (2004) 3D Slicer. Biomedical Imaging: Nano to Macro, 2004. IEEE International Symposium:32–635
35. Plesnila N (2007) Decompression craniectomy after traumatic brain injury: recent experimental results. Prog Brain Res 161:393–400
36. Rieth KG, Fujiwara K, Di Chiro G, Klatzo I, Brooks RA, Johnston GS, O'Connor CM, Mitchell LG (1980) Serial measurements of CT attenuation and specific gravity in experimental cerebral edema. Radiology 135:343–348
37. Rózsa L, Grote EH, Egan P (1989) Traumatic brain swelling studied by computerized tomography and densitometry. Neurosurg Rev 12:133–140
38. Schneider GH, Bardt T, Lanksch WR, Unterberg A (2002) Decompressive craniectomy following traumatic brain injury: Icp, cpp and neurological outcome. Acta Neurochir Suppl 81:77–79
39. Servadei F (2011) Clinical value of decompressive craniectomy. N Engl J Med 364:1558–1559
40. Smith DH, Meaney DF (2000) Axonal damage in traumatic brain injury. Neuroscientist 6:483–495
41. Staal JA, Dickson TC, Gasperini R, Liu Y, Foa L, Vickers JC (2010) Initial calcium release from intracellular stores followed by calcium dysregulation is linked to secondary axotomy following transient axonal stretch injury. J Neurochem 112:1147–1155
42. Stiver SI (2009) Complications of decompressive craniectomy for traumatic brain injury. Neurosurg Focus 26:E7
43. Stocchetti N, Colombo A, Fetal O (2007) Time course of intracranial hypertension after traumatic brain injury. J Neurotrauma 24:1339–1346
44. Szczygielski J, Mautes AE, Schwerdtfeger K, Steudel WI (2010) The effects of selective brain hypothermia and decompressive craniectomy on brain edema after closed head injury in mice. Brain Edema XIV:225–229
45. Tang-Schomer MD, Patel AR, Baas PW, Smith DH (2010) Mechanical breaking of microtubules in axons during dynamic

stretch injury underlies delayed elasticity, microtubule disassembly, and axon degeneration. FASEB J 24:1401–1410
46. Timmons SD, Ullman JS, Eisenberg HM, Romero CM, Simard JM, Kahle KT, Walcott BP, Hautefeuille S, Francony G, Payen JF et al (2011) Craniectomy in diffuse traumatic brain injury. N Engl J Med 365:373–376
47. Timofeev I, Kirkpatrick PJ, Corteen E, Hiler M, Czosnyka M, Menon DK, Pickard JD, Hutchinson PJ (2006) Decompressive craniectomy in traumatic brain injury: outcome following protocol-driven therapy. Acta Neurochir Suppl 96:11–16
48. Tomura S, Nawashiro H, Otani N, Uozumi Y, Toyooka T, Ohsumi A, Shima K (2011) Effect of decompressive craniectomy on aquaporin-4 expression after lateral fluid percussion injury in rats. J Neurotrauma 28:237–243
49. Unterberg AW, Stover J, Kress B, Kiening KL (2004) Edema and brain trauma. Neuroscience 129:1019–1027
50. Vashu R, Sohail A (2011) Decompressive craniectomy is indispensible in the management of severe traumatic brain injury. Acta Neurochir (Wein) 10:2065–2066
51. Vercauteren T, Pennec X, Perchant A, Ayache N (2009) Diffeomorphic demons: Efficient non-parametric image registration. NeuroImage 45:S61–S72
52. Veress AI, Gullberg GT, Weiss JA (2005) Measurement of strain in the left ventricle during diastole with cine-mri and deformable image registration. J Biomech Eng 127:1195–1207
53. Von Holst H (2007) Traumatic brain injury. In: Feigin VL, Bennett DA (eds) Handbook of clinical neuroepidemiology. Nova Science, New York, pp 197–232
54. Wirtz CR, Steiner T, Aschoff A, Schwab S, Schnippering H, Steiner HH, Hacke W, Kunze S (1997) Hemicraniectomy with dural augmentation in medically uncontrollable hemispheric infarction. Neurosurg Focus 2:Article 3
55. Yu Z, Morrison B (2010) Experimental mild traumatic brain injury induces functional alteration of the developing hippocampus. J Neurophysiol 103:499–501
56. Zweckberger K, Erös C, Zimmermann R, Kim SW, Engel D, Plesnila N (2006) Effect of early and delayed decompressive craniectomy on secondary brain damage after controlled cortical impact in mice. J Neurotrauma 23:1083–1093